Electronic Supplementary Information for

Spatial porosity design of Fe-N-C catalyst for high power density PEM fuel cells and detection of water saturation of catalyst layer by a microwave method

Lu Chen,‡[a] Xin Wan,‡[a] Xiaonan Zhao,[a] Wenwen Li,[a] Xiaofang Liu,*[a] Lirong Zheng,[b] Qingtao Liu,[a] Ronghai Yu[a] and Jianglan Shui*[a]

[a]School of Materials Science and Engineering, Beihang University, Beijing 100191, China

[b]Beijing Synchrotron Radiation Facility, Institute of High Energy Physics, Chinese Academy of Sciences, Beijing, 100049, China

*Corresponding authors.

E-mail addresses: liuxf05@buaa.edu.cn (X. Liu), shuijianglan@buaa.edu.cn (J. Shui).

‡These authors contributed equally to this work.

Experimental Section

Synthesis of ZIF-8

In a typical procedure, methanol solution (200 ml) containing $Zn(NO_3)_2 \cdot 6H_2O$ (5.88 g) was quickly poured into another methanol solution (200 ml) containing 2-methylimidazole (6.48 g) under stirring. The mixture was stirred for 2 h at room temperature. The white suspension was centrifuged, washed with methanol four times and dried in vacuum at 60 °C overnight.

Synthesis of SM-NC

ZIF-8 particles were first coated with a layer of silica with a thickness of about 15 nm[1]. ZIF-8 (300 mg) was dispersed in H_2O (120 ml), and then NaOH solution (4.8 ml, 6 mg ml^{-1}) and cetyltrimethylammonium bromide solution (3 ml, 25 mg ml^{-1}) were added. The mixture was stirred for 0.5 h at room temperature. Tetraethyl orthosilicate (0.6 ml in 3 ml of methanol) was injected into the above solution, and the dispersion was stirred for 1 h. The resulting ZIF-8@SiO_2 core-shell nanoparticles were collected by centrifugation and washed with ethanol and dried in vacuum at 60 °C overnight. Subsequently, ZIF-8@SiO_2 (300 mg) and NaCl (1 g) were dispersed in H_2O (30 mL) with stirring for 0.5 h at room temperature. The powder was collected by filtration and washed with deionized water, dried in vacuum at 60 °C overnight, and then pyrolyzed at 1000 °C for 1 h under argon atmosphere in a tube furnace. Then, the silica layer was etched off in 3 M NaOH solution at 50 °C for 20 h, and then the dispersion was separated by filtration and washed thoroughly until the filtrate became neutral to obtain surface mesoporous nitrogen-doped carbon nanoparticles, denoted as SM-NC.

Synthesis of MesoS/MicroC-FeNC

SM-NC (50 mg) was dispersed in H_2O (50 ml), which was ultra-sonicated for 0.5 h. Then $FeCl_3 \cdot 6H_2O$ solution (1.25 ml, 5 mg ml^{-1}) was dropwise added into the SM-NC suspension. After stirring for 1 h at room temperature, the suspension was heated at 70 ºC for 8 h. Then, SM-NC particles with adsorbed Fe^{3+} were thoroughly washed and collected by filtration, dried in vacuum at 60 ºC overnight and then pyrolyzed at 1000 °C for 1 h under argon atmosphere. When the temperature decreased to 800 °C, ammonia (200 $ml \cdot min^{-1}$) was introduced into the tube (diameter of 5 cm), and the furnace was kept at this temperature for 20 min. Subsequently, the ammonia was switched to argon and the furnace was cooled down to room temperature. The obtained powder is the final catalyst MesoS/MicroC-FeNC.

Synthesis of Meso-FeNC, Micro-FeNC and NC

For Micro-FeNC, the as-obtained ZIF-8 powder (300 mg) was firstly heated at 1000 °C for 1 h to obtain nitrogen-doped carbon particles. The following procedures of Fe^{3+} ion adsorption and heat treatment are identical to the synthesis of MesoS/MicroC-FeNC. The synthesis of Meso-FeNC is identical to the synthesis of MesoS/MicroC-FeNC except that the brine-etching duration lasted 1 h. For NC, the procedure is identical to the synthesis of SM-NC, representing a metal-free catalyst without iron functionalization.

Characterization

The morphology was investigated by scanning electron microscopy (SEM, JEOL, JSM-7500). Transmission electron microscopy (TEM) observation and energy

dispersive spectroscopy (EDS) elemental mapping characterization were performed with JEOL-2100F with the electron acceleration energy of 200 kV. The images of single iron atoms were obtained by a high-angle annular dark-filed scanning transmission electron microscopy (HAADF-STEM, Titan Cubed Themis G2 300) operated at 200 kV. The N_2 adsorption and desorption isothermals were acquired on an AS-6B system (Quantachrome Instruments) at the temperature of 77.3 K. The specific surface area was obtained using the Brunauer-Emmett-Teller method. The external surface area is defined as the non-micropore area, which is obtained by subtracting the micropore surface area from the Brunauer-Emmett-Teller surface area. The X-ray diffraction (XRD) patterns were recorded using a Rigaku D/max 2500 with Cu Kα irradiation. X-ray photoelectron spectroscopy (XPS) measurements were collected using ESCALAB 250Xi with Al Kα irradiation. XAS was performed at room temperature on the 1W1B beamline at Beijing Synchrotron Radiation Facility (BSRF). Transmissive-mode Fe K-edge X-ray absorption spectra were collected for MesoS/MicroC-FeNC over a range of 6974–8110 eV, where a 100% Ar filled Lytle ion-chamber detector with Mn X-ray filters and soller slits were used. The monochromator energy was calibrated using a Fe foil. The XAFS data were analyzed using IFEFFIT. Least-squares curve fitting was carried out to get the quantitative structural parameters around iron atoms, using the ARTEMIS program[2].

Rotating ring disk electrode tests

The ORR activity of the catalyst was measured in 0.5 M H_2SO_4 (or 0.1 M $HClO_4$ for Pt/C) on a glassy carbon rotating ring disk electrode (RRDE, 5.61 mm of disk outer

diameter, Pine Research Instrumentation, USA) with an electrochemical workstation (CHI 760E, CH Instruments). The reference electrode was a calibrated saturated calomel electrode, and a graphite rod was used as the counter electrode. All of the potentials reported were calibrated to the reversible hydrogen electrode. For the catalyst ink preparation, catalyst (5 mg), Nafion alcohol (5 wt%, Aldrich; 10 μl), deionized water (215 μl) and isopropanol (275 μl) were mixed and then sonicated to a uniform suspension. Before loading the catalyst, the glassy carbon electrode was polished and rinsed with deionized water. The ink (10 μl) containing 100 μg of catalysts was pipetted onto the glassy carbon and dried in air, resulting in a catalyst loading of around 400 μg cm^{-2}. Pt/C(20 wt%) catalyst with a loading of 40 μg Pt cm^{-2} was used as a reference. Experiments were conducted at room temperature (~25 °C). The electrolyte was purged by any specific gas at least 30 min before the test and the gas flow was maintained during the experiment. The capacitive background was firstly obtained in the Ar-purged electrolyte by potential sweep at a scan rate of 10 mV s^{-1}. Afterwards, the electrolyte was purged with O_2, followed by linear sweep voltammetry (LSV) at the same scan rate for ORR activity tests. The oxygen reduction currents were obtained by subtracting the background current from the original LSV measured in the O_2-saturated electrolyte. Tests were performed at 1600 rpm. The peroxide yields (H_2O_2%) were calculated from the ring current (I_r) and the disk current (I_d) using the equation:

$$H_2O_2\% = 200 \times I_r/(I_r + NI_d) \quad (1)$$

The electron transfer number (n) in acid was calculated by the equation:

$$n = 4I_d/(I_d + I_r/N) \quad (2)$$

where $N = 0.37$ is the current collection efficiency of the Pt ring.

PEMFC tests

The Fe-N-C catalyst (~15 mg) was mixed with Nafion alcohol solution (5 wt%, Aldrich), deionized water (200 mg) and isopropanol (400 mg) to prepare the catalyst ink. The weight ratio of Nafion/catalyst (NCR) is 1:1. The ink was subjected to sonication for 30 min and stirring for 10 h to make a uniform suspension. The ink was brushed on a piece of carbon paper (5 cm^2, Ballard GDS2240), followed by drying in vacuum at 80 °C for 2 h to obtain the cathoode. Pt/C (40 wt% of Pt, BASF) with a loading of ~0.2 mg_{Pt} cm^{-2} on carbon paper was used as anode. The 40 wt% Pt/C (~3 mg) was mixed with Nafion alcohol solution (5 wt%, 60 mg), deionized water (100 mg) and isopropanol (200 mg) to prepare the catalyst ink. The ink was subjected to sonication for 10 min and stirring for 1 h to make a uniform suspension. The ink was brushed on a piece of carbon paper (5 cm^2), followed by drying in vacuum at 80 °C for 2 h to obtain the anode. The prepared cathode and anode were pressed onto the two sides of a Nafion 211 membrane (Dupont) at 130 °C for 90 s under a pressure of 1.5 MPa to obtain the membrane electrode assembly (MEA). A control MEA of Pt/C catalysts was prepared in the similar way with 0.2 mg_{Pt} cm^{-2} Pt/C (40%, BASF) on both cathode and anode. The MEA was measured by a fuel cell test station (Scribner 850e) with UHP-grade H_2 and O_2 at 80 °C, 100% RH. The flow rate was 0.3 L min^{-1} for H_2 and 0.4 L min^{-1} for O_2. The absolute gas pressure was 1.5 bar.

Quantification of the active sites

According to the work reported by Kucernak *et al*[3], the site density (*SD*) can be obtained by nitrite adsorption and desorption method. Firstly, repetitive cycling in pH 5.2 acetate buffer alternatively in O_2 and N_2 was implemented to exclude the error induced by the testing environment. The linear sweep voltammetry and cyclic voltammetry curves were recorded before, during and after the nitrite absorption. Then the catalyst was poisoned by $NaNO_2$ and nitrite stripping was conducted subsequently. *SD* was proportional to the excess in cathodic charge (Q_{strip}) and can be calculated by the equation:

$$SD\ (mol\ g^{-1}) = \frac{Q_{strip}\ (C\ g^{-1})}{n_{strip}\ F\ (C\ mol^{-1})} \tag{3}$$

where n_{strip} (= 5) is the number of electrons associated with the reduction of one nitrite per site. *F* is Faraday's constant.

Permittivity measurements

To avoid the interference of carbon paper, the decal transfer method was introduced to separate the catalyst layer and the gas diffusion layer. The cathode and anode catalyst inks were sprayed onto the PTFE substrate and hot-pressed onto two separate pieces of a Nafion 211 membrane, which were later put together with two pieces of carbon paper to form a two-layer membrane-electrode assembly (MEA). This approach facilitated the permittivity measurement of the individual catalyst layer with minimal interference (only with the membrane). The as-prepared MEA was scanned from open circuit voltage (OCV) to various potentials (0.8 and 0.5 V) and then the catalyst layer coated on the membrane was taken out for permittivity measurement. The electromagnetic parameters of the catalyst layers were measured by a vector network analyzer (N5234B

PNA-L, KEYSIGHT) in the frequency range of 8.2–12.4 GHz. The cathode catalyst layer has a size of 23 x 23 x 0.07 mm^3, while the sample holder has an opening of 22.86 x 10.16 mm^2. To ensure comparable results, the area is fixed for each measurement. Before the measurement, a standard calibration process was performed.

Supplementary Figures and Tables

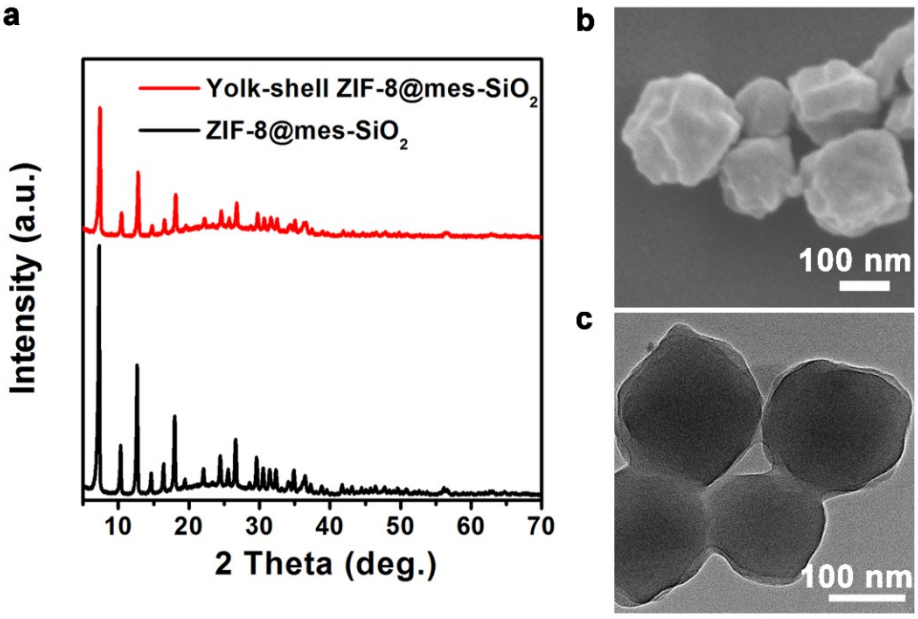

Fig. S1. (a) XRD patterns of ZIF-8@mes-SiO_2 and brine washed ZIF-8@mes-SiO_2, showing the intact ZIF-8 crystal structure after the brine wash. (b) SEM image and (c) TEM image of residual yolk-shell structured ZIF-8 after removing the SiO_2 shell from the ZIF-8@mes-SiO_2 by 3 M NaOH solution.

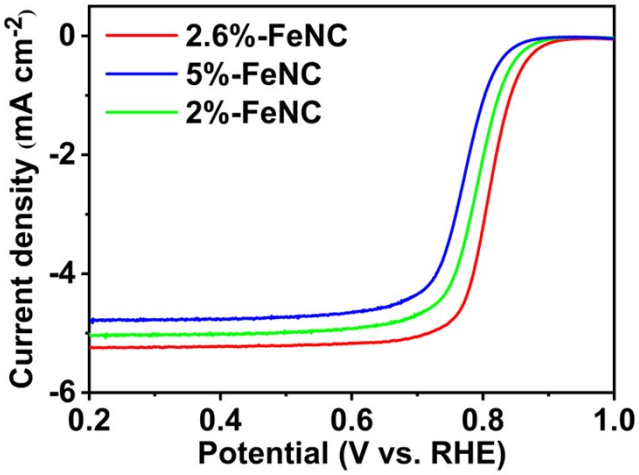

Fig. S2. LSV curves of MesoS/MicroC-FeNC with different additions of iron in the catalysts in O_2-saturated 0.5 M H_2SO_4. The weight percentage of 2.6%, 5% and 2% refers to the weight percent of SM-NC. The Fe concentration of 2.6%-FeNC is 2.47 wt% determined by ICP.

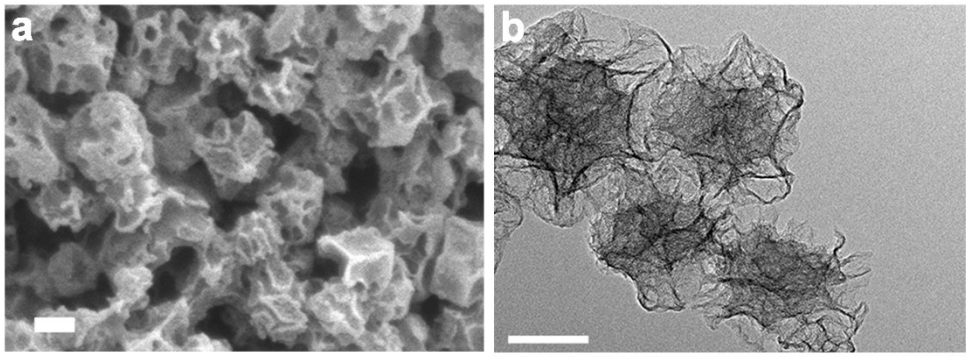

Fig. S3. SEM and TEM images of MesoS/MicroC-FeNC particles clearly show a relatively dense core in each particle. Scale bars: 100 nm.

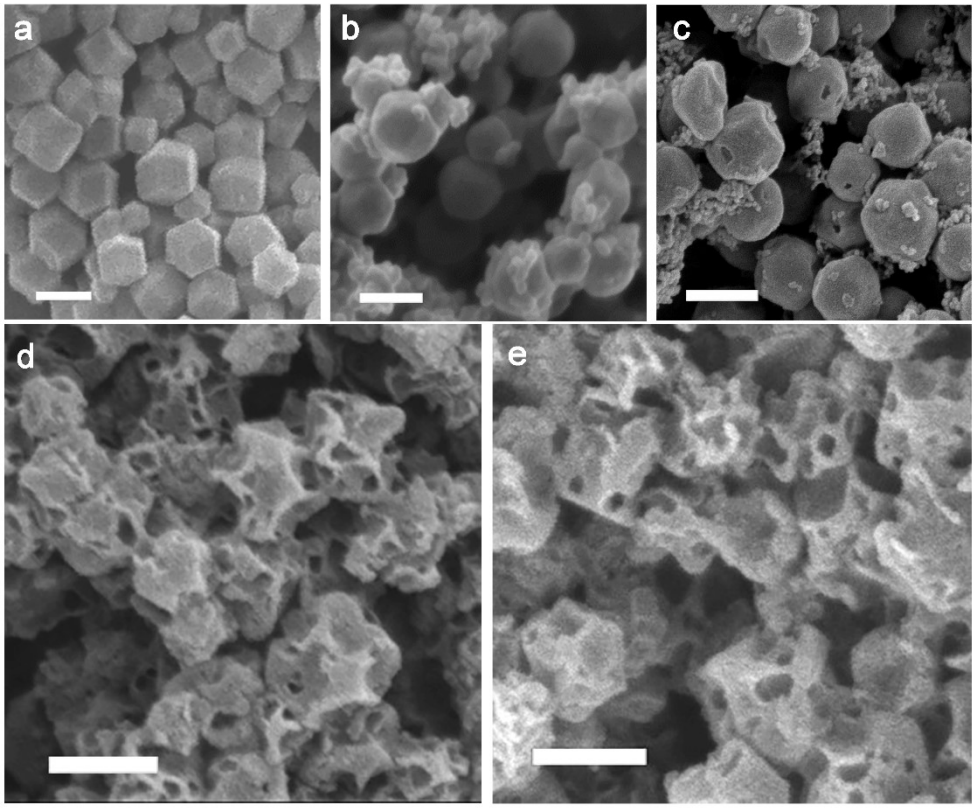

Fig. S4. Morphology evolution of MesoS/MicroC-FeNC during the synthesis. SEM images of (a) ZIF-8, (b) ZIF-8@mes-SiO_2, (c) yolk-shell ZIF-8@mes-SiO_2, (d) SM-NC, and (e) MesoS/MicroC-FeNC. Scale bars: 200 nm.

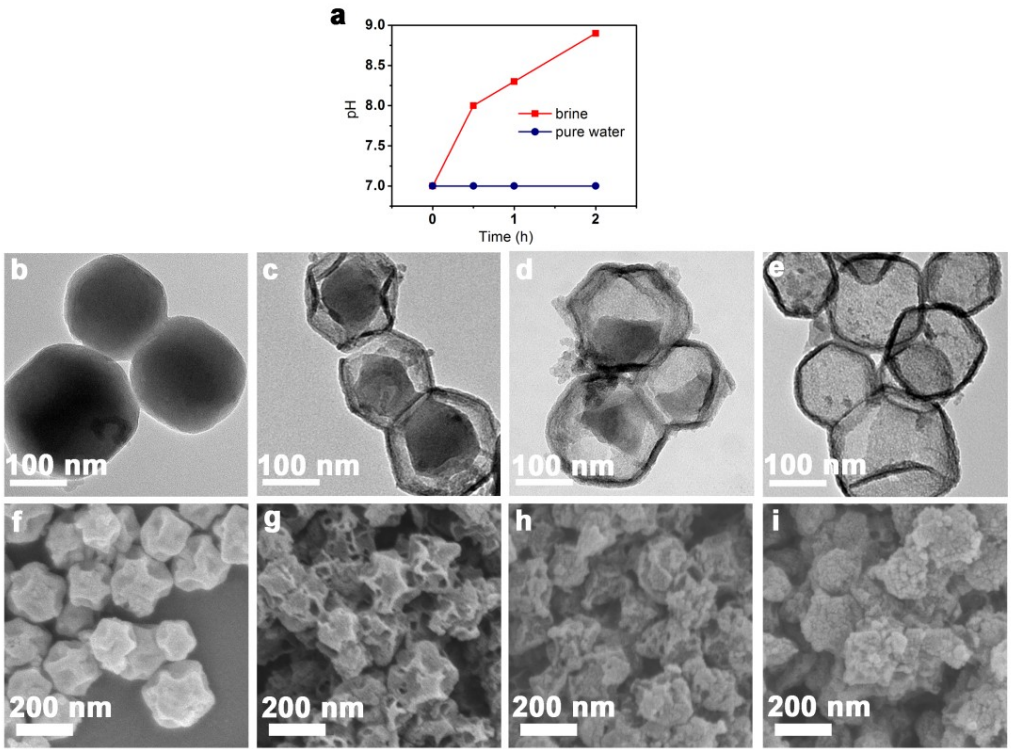

Fig. S5. (a) The pH values of the NaCl solution and water after washing ZIF-8 for the indicated durations. TEM images of brine washed ZIF-8@SiO_2 at durations of (b) 0 h, (c) 0.5 h, (d) 1 h and (e) 2 h. SEM images of the materials after carbonization and removal of SiO_2: (f) 0 h, (g) 0.5 h, (h) 1 h and (i) 2 h.

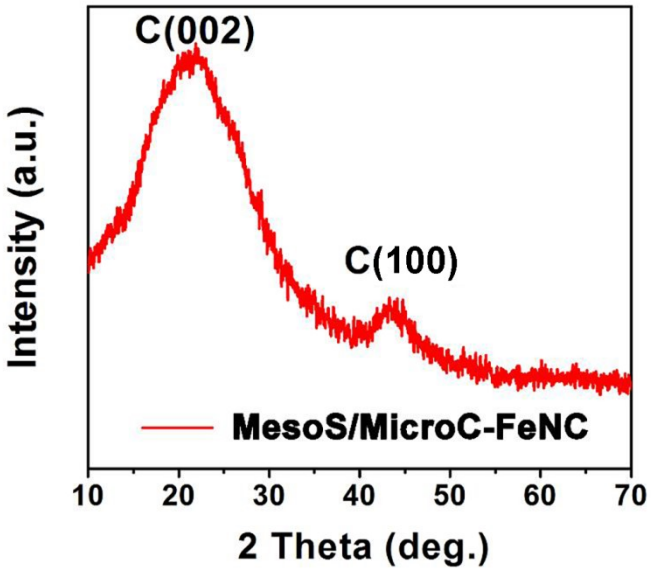

Fig. S6. XRD pattern of MesoS/MicroC-FeNC.

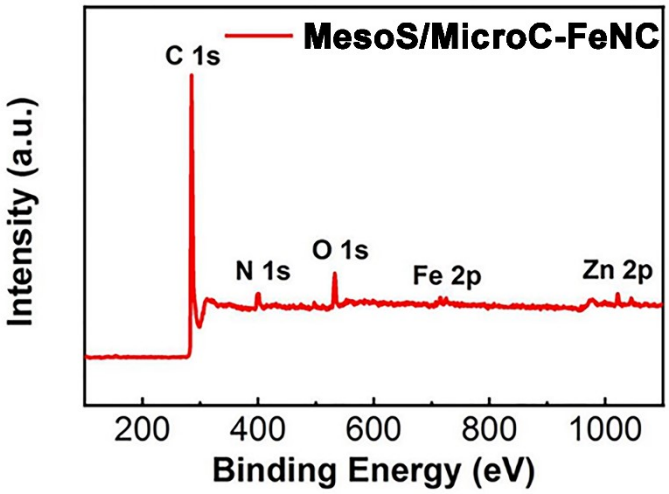

Fig. S7. XPS survey spectrum of MesoS/MicroC-FeNC.

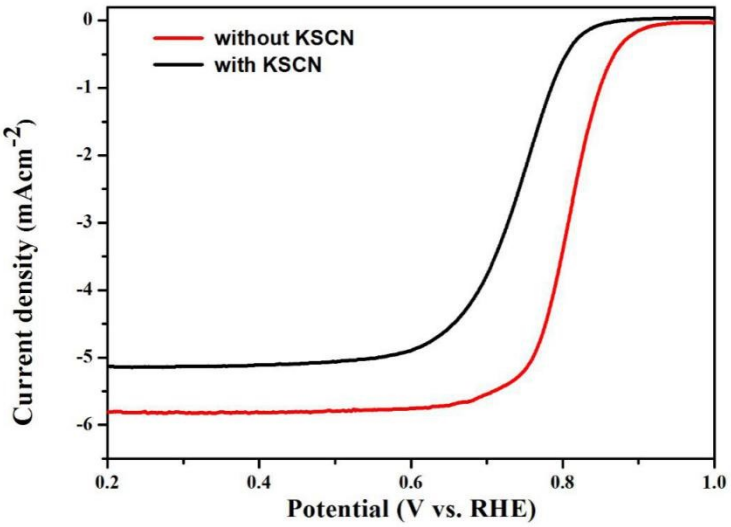

Fig. S8. LSV curves of MesoS/MicroC-FeNC in O_2-saturated 0.5 M H_2SO_4 with and without KSCN, respectively.

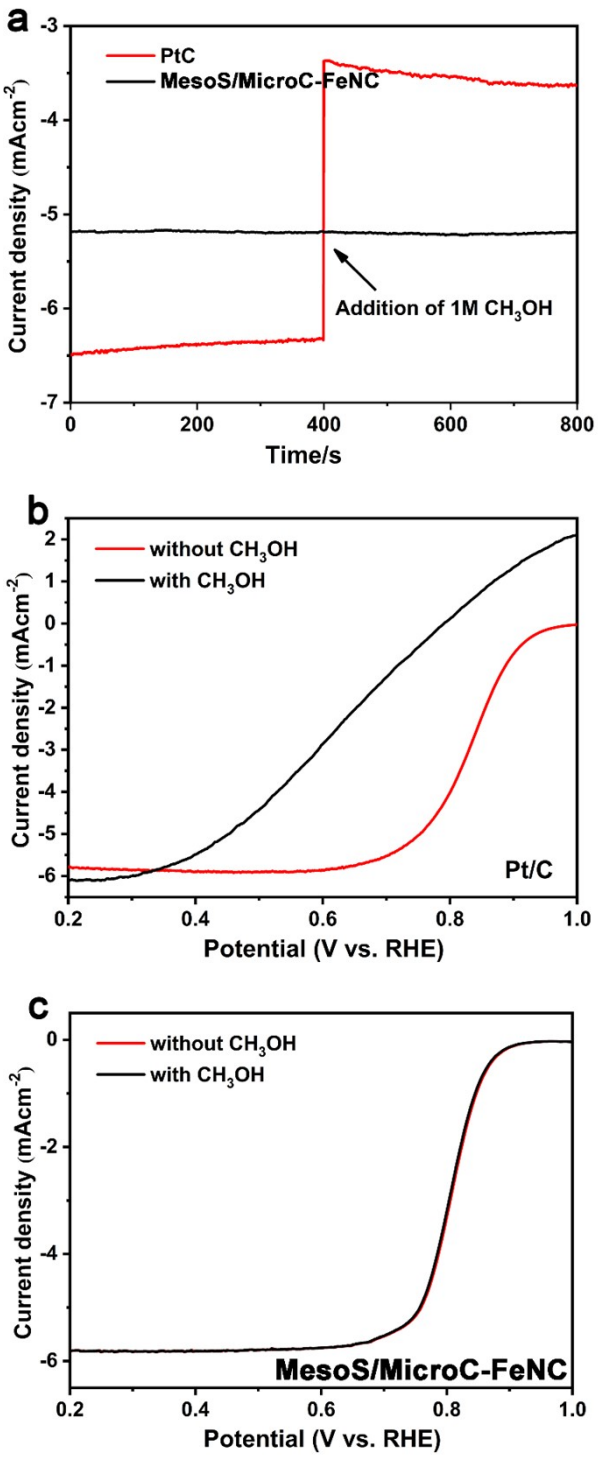

Fig. S9. (a) Current density–time curves of MesoS/MicroC-FeNC in 0.5 M H_2SO_4 and Pt/C in 0.1 M $HClO_4$ with the addition of methanol. LSV curves of (b) MesoS/MicroC-FeNC and (c) Pt/C in O_2-saturated 0.5 M H_2SO_4 with and without methanol, respectively.

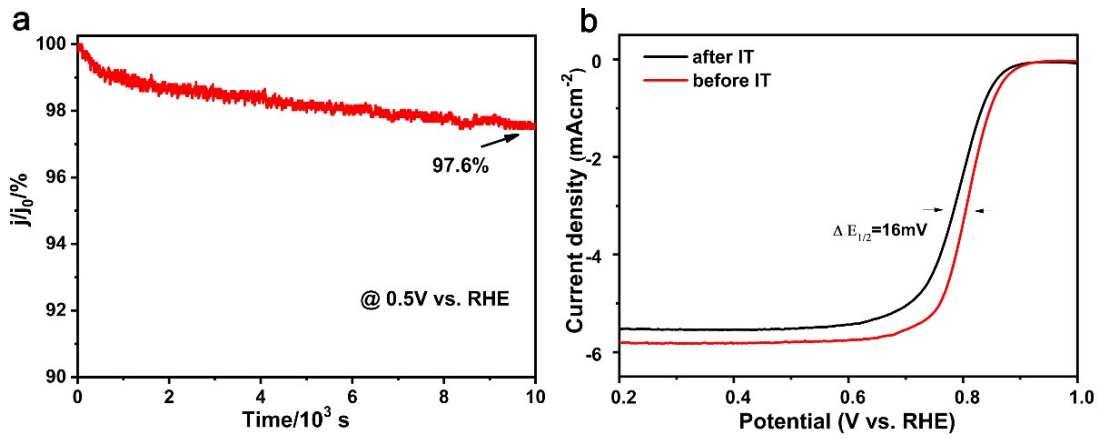

Fig. S10. (a) Current-time (IT) chronoamperometric response of MesoS/MicroC-FeNC at 0.5 V (vs. RHE) in O_2-saturated 0.5 M H_2SO_4. (b) LSV curves before and after the IT test.

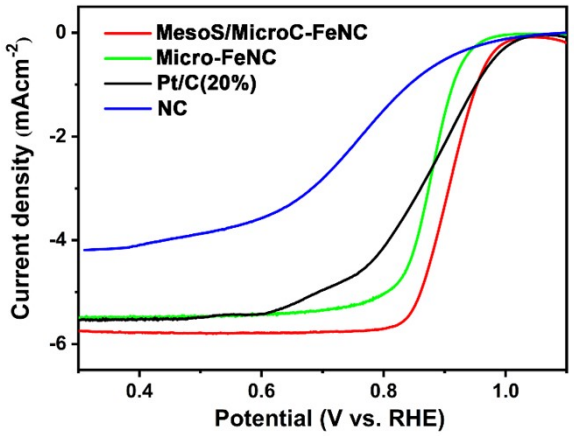

Fig. S11. LSV curves of the indicated catalysts in O_2-saturated 0.1 M KOH.

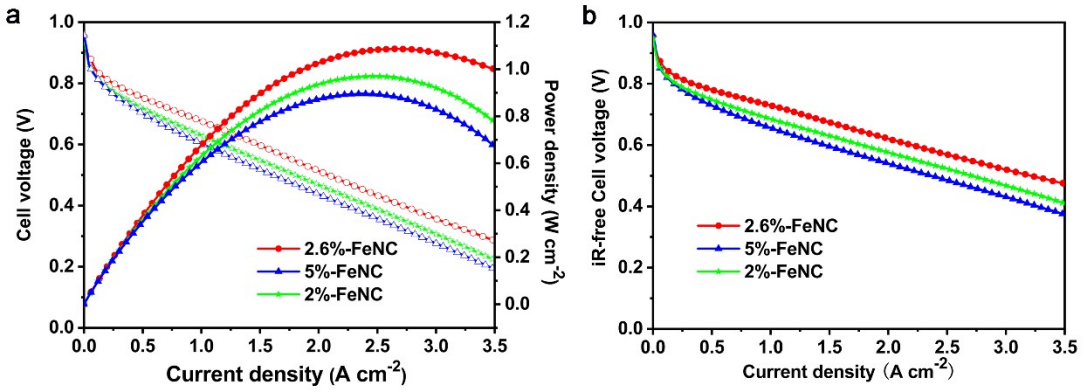

Fig. S12. PEMFC performance of MesoS/MicroC-FeNC catalysts with the indicated additions of iron. (a) Polarization curves and power density curves, (b) internal resistance compensated polarization curves. Test conditions: cathode loading 2.7 mg cm^{-2}, Pt/C anode loading 0.2 mg_{Pt} cm^{-2}, Nafion 211 membrane, 5 cm^2 electrode area, 80 °C, 100%RH, 1.5 bar H_2-O_2.

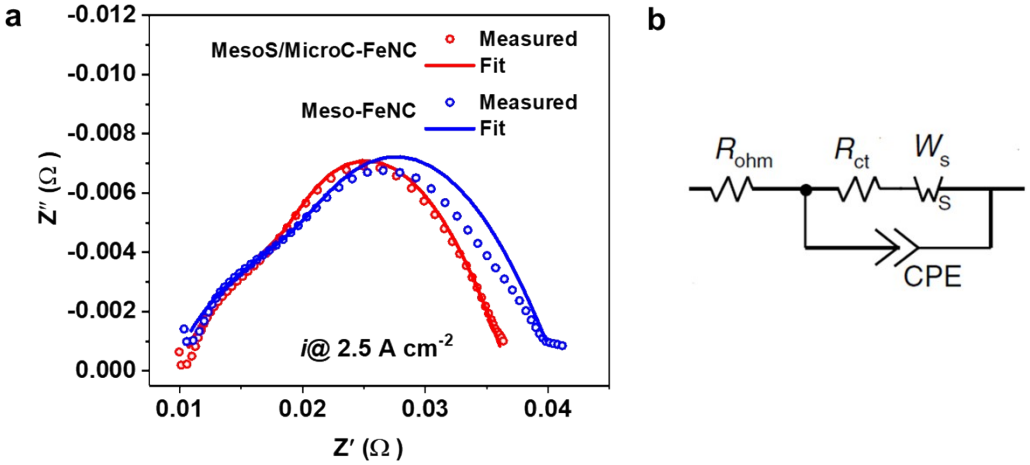

c

Catalyst	R_Ω / Ω	R_{ct} / Ω	W_s-R / Ω
MesoS/MicroC-FeNC	0.010	0.013	0.013
Meso-FeNC	0.009	0.015	0.016

Fig. S13. (a) Nyquist plots for PEMFCs of indicated cathode catalysts at the current density of 2.5 A cm^{-2}. *Z′* and *Z″* are the real and imaginary parts of the impedance. (b) The equivalent circuit model. (c) Fitting results of the EIS curves.

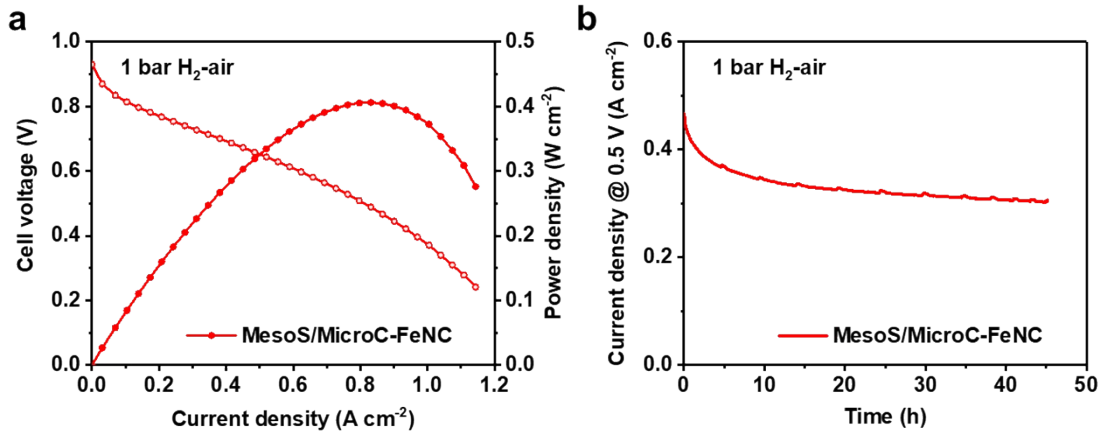

Fig. S14. (a) Polarization and power density curves of MesoS/MicroC-FeNC cathode at loading of 2.7 mg cm^{-2} under 1 bar H_2-air at flow rates of 300/500 ml min^{-1}. (b) A 45-h stability test of MesoS/MicroC-FeNC cathode under 1 bar H_2-air at flow rates of 100/100 ml min^{-1}.

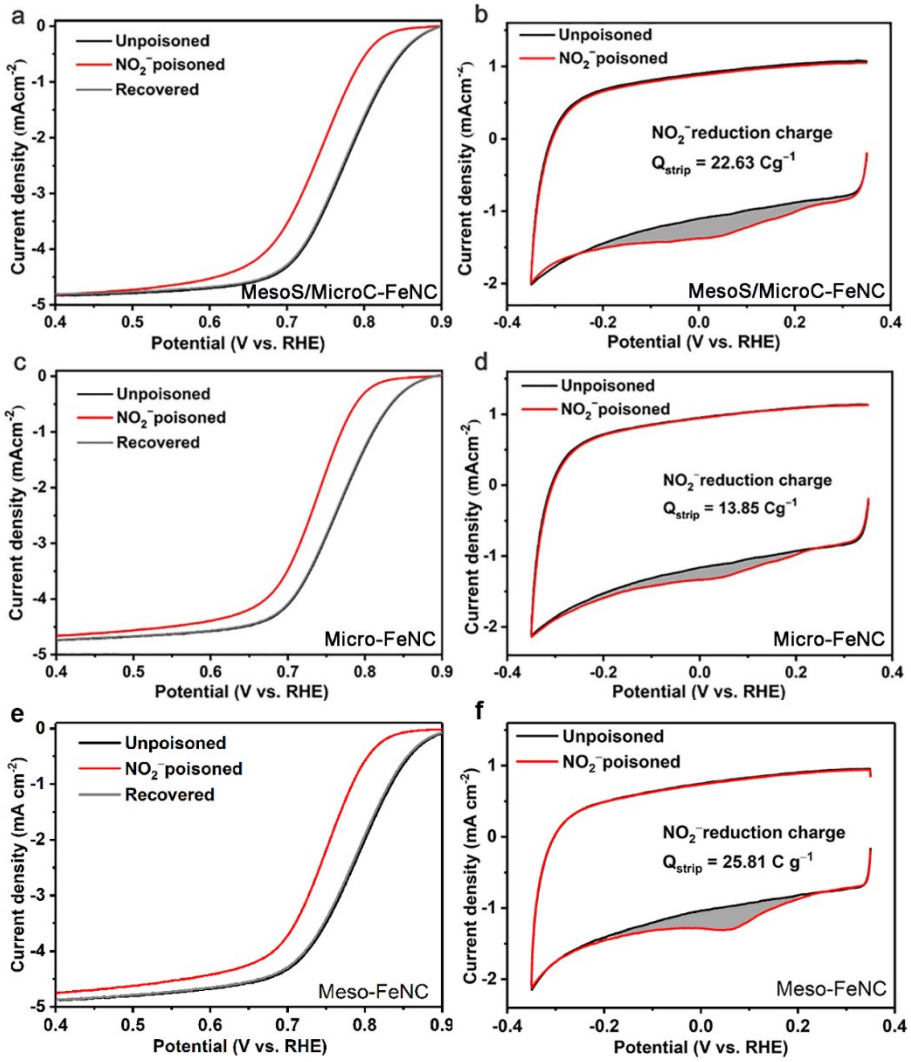

Fig. S15. Accessible active site density measurements of MesoS/MicroC-FeNC, Micro-FeNC and Meso-FeNC. (a, c, e) LSV curves before, during and after nitrite adsorption in a 0.5 M acetate buffer at pH 5.2. (b, d, f) CV curves before and during nitrite adsorption in the nitrite reductive stripping region. Catalyst loading, 0.27 mg cm^{-2}. Since the accessible Fe-N_4 sites are poisoned by nitrite anions, the number of active sites can be indicated as the number of adsorbed nitrite anions which are stripped to recover the catalytic activity with a transfer of 5 electrons per nitrite anion. The Q_{strip} is the excess coulometric charge related to the stripping of nitrite anions.

Table S1. Porosity of Micro-FeNC, MesoS/MicroC-FeNC and Meso-FeNC.

Sample	S_{BET} / $m^2\ g^{-1}$	Mesopore surface area / $m^2\ g^{-1}$	Mesopore volume / $cm^3\ g^{-1}$
Micro-FeNC	1105	146	0.094
MesoS/MicroC-FeNC	1145	485	0.653
Meso-FeNC	1408	551	0.763

Table S2. EXAFS data fitting results of MesoS/MicroC-FeNC.

Path	***N***	***R*/Å**	**σ^2 / 10^{-3} Å^2**	**ΔE_0 / eV**	**S_0^2**	**R-factor**
Fe-N/O	6	2.00	9.86	−1.15	0.78	0.003

N, coordination number; R, distance between absorber and backscatter atoms; σ^2, Debye-Waller factor to measure thermal and static disorder in absorber-scatter distances; ΔE_0, inner potential correction; R-factor is used to value the goodness of fitting.

Table S3. Maximum power density comparison in H_2-O_2 PEMFC.

Catalyst	**P_{max} (mW cm^{-2})**	**Absolute Pressure (bar)**	**T_{cell} (°C)**	**Loading (mg cm^{-2})**	**Year**	**Ref.**
1MIL/40ZIF-1000	760	1	80	0.5	2019	[4]
S-Fe/Z8/2-AT(16.4)	800	1	80	4	2018	[5]
MesoS/MicroC-FeNC	1080	1.5	80	2.7		**This work**
MgO@Phen-Fe-800-3/1	630	1.5	70	3	2019	[6]
ZIF'-FA-CNT-P	820	1.5	80	4.5	2017	[7]
Fe-NMCSs	463	1.5	80	4	2016	[8]
ZIF-8/TPI	620	1.5	80	2.2	2014	[9]
Fe/TPTZ/ZIF-8	750	1.5	80	4	2013	[10]
Fe-N-C-Phen-PANI	1.06	1.9	80	4	2017	[11]
FeNC-1000	1010	2	80	2	2019	[12]
Fe/N/C-SiO_2-$ZnCl_2$	600	2.5	80	2	2018	[13]
TPI@Z8(SiO_2)-650-C	1180	2.5	80	2.8	2019	[14]
Fe2-Z8-C	1141	2.5	80	2.8	2018	[15]

Table S4. Surface elemental composition of catalysts determined by XPS.

	C% (at/wt)	N% (at/wt)	O% (at/wt)	Fe% (at/wt)	Zn% (at/wt)*
MesoS/MicroC-FeNC	92.01/88.53	4.18/4.69	3.29/4.22	0.21/0.94	0.31/1.62
Micro-FeNC	91.46/87.69	3.85/4.31	4.14/5.29	0.20/0.89	0.35/1.82

*It is normal to remain a small amount of zinc in this kind of ZIF8-derived catalyst, which may present in the form of Zn-N_4. However, based on our electrochemical tests, these Zn-based sites contribute negligible ORR activity in acid.

Supplementary References:

1. L. Shang, H. Yu, X. Huang, T. Bian, R. Shi, Y. Zhao, G. I. Waterhouse, L. Z. Wu, C. H. Tung and T. Zhang, *Adv. Mater.*, 2016, **28**, 1668–1674.
2. B. Ravel and M. Newville, *J. Synchrotron Radiat.*, 2005, **12**, 537–541.
3. D. Malko, A. Kucernak and T. Lopes, *Nat. Commun.*, 2016, **7**, 13285.
4. H. Wang, F. X. Yin, N. Liu, R. H. Kou, X. B. He, C. J. Sun, B. H. Chen, D. J. Liu and H. Q. Yin, *Adv. Funct. Mater.*, 2019, **29**, 1901531.
5. Y. J. Wu, Y. C. Wang, R. X. Wang, P. F. Zhang, X. D. Yang, H. J. Yang, J. T. Li, Y. Zhou, Z. Y. Zhou and S. G. Sun, *ACS Appl. Mater. Interfaces*, 2018, **10**, 14602–14613.
6. Y. Zhan, H. Zeng, F. Xie, H. Zhang, W. Zhang, Y. Jin, Y. Zhang, J. Chen and H. Meng, *J. Power Sources*, 2019, **431**, 31–39.
7. C. Zhang, Y. C. Wang, B. An, R. Huang, C. Wang, Z. Zhou and W. Lin, *Adv. Mater.*, 2017, **29**, 1604556.
8. F. L. Meng, Z. L. Wang, H. X. Zhong, J. Wang, J. M. Yan and X. B. Zhang, *Adv. Mater.*, 2016, **28**, 7948–7955.
9. D. Zhao, J. L. Shui, L. R. Grabstanowicz, C. Chen, S. M. Commet, T. Xu, J. Lu and D. J. Liu, *Adv. Mater.*, 2014, **26**, 1093–1097.
10. J. Tian, A. Morozan, M. T. Sougrati, M. Lefevre, R. Chenitz, J. P. Dodelet, D. Jones and F. Jaouen, *Angew. Chem. Int. Ed.*, 2013, **52**, 6867–6870.
11. X. Fu, P. Zamani, J. Y. Choi, F. M. Hassan, G. Jiang, D. C. Higgins, Y. Zhang, M. A. Hoque and Z. Chen, *Adv. Mater.*, 2017, **29**, 1604456.
12. Y. Li, X. Liu, L. Zheng, J. Shang, X. Wan, R. Hu, X. Guo, S. Hong and J. Shui, *J. Mater. Chem. A*, 2019, **7**, 26147–26153.
13. R. Wu, Y. Song, X. Huang, S. Chen, S. Ibraheem, J. Deng, J. Li, X. Qi and Z. Wei, *J. Power Sources*, 2018, **401**, 287–295.
14. X. Wan, X. Liu, Y. Li, R. Yu, L. Zheng, W. Yan, H. Wang, M. Xu and J. Shui, *Nat. Catal.*, 2019, **2**, 259–268.
15. Q. Liu, X. Liu, L. Zheng and J. Shui, *Angew. Chem. Int. Ed.*, 2018, **57**, 1204–1208.